

# Entanglement and Entropy Engineering of Atomic Two-Qubit States

S. G. Clark and A. S. Parkins\*

*Department of Physics, University of Auckland, Private Bag 92019, Auckland, New Zealand.*

(Dated: October 26, 2018)

We propose a scheme employing quantum-reservoir engineering to controllably entangle the internal states of two atoms trapped in a high finesse optical cavity. Using laser and cavity fields to drive two separate Raman transitions between metastable atomic ground states, a system is realized corresponding to a pair of two-state atoms coupled collectively to a squeezed reservoir. Phase-sensitive reservoir correlations lead to entanglement between the atoms, and, via local unitary transformations and adjustment of the degree and purity of squeezing, one can prepare entangled mixed states with any allowed combination of linear entropy and entanglement of formation.

PACS numbers: 03.65.Ud, 03.67.-a, 42.50.-p

The properties of entangled mixed states and schemes for their controlled preparation are presently under vigorous investigation, primarily because of their relevance to understanding the role of purity and entanglement in quantum information protocols such as quantum computation and quantum communication [1]. The purity and degree of entanglement of two-qubit states can be quantified, respectively, by the linear entropy and either the entanglement of formation or the concurrence [2]. Here, we propose a scheme using interactions in cavity quantum electrodynamics (cavity QED) which enables the preparation of states of two atomic qubits with *any* allowed combination of linear entropy and concurrence.

Our scheme uses the technique of quantum-reservoir engineering [3] in a cavity QED setting to couple a pair of two-state atoms collectively to an effective squeezed reservoir. The phase-sensitive quantum correlations of the reservoir are transferred to the two-atom system to produce entangled atomic states [4, 5]. The degrees of purity and entanglement of the atomic states can be controlled through the excitation time, through properties of the effective squeezing (i.e., the degree and purity of squeezing), and through adjustment of the relative strengths of amplitude and phase coupling to the reservoir. We are thus able to scan the entire allowed region of the linear entropy–concurrence plane (or linear entropy–tangle plane [2]), including the region between the Werner states [6] and the recently characterized maximally-entangled mixed states (MEMS) [2]. Other cavity-QED-based schemes for entangling a pair of atoms have been proposed and even implemented (see, e.g., [7, 8, 9]), but these schemes have focussed primarily on generating maximally-entangled pure states.

In our proposal, two atoms are assumed to be tightly confined inside a high-finesse optical cavity and separated by a distance that is sufficiently large that they can be individually addressed by probe lasers and so that there is no direct dipole-dipole interaction between them. The cavity has a field decay rate of  $\kappa$  and a frequency  $\omega$ , and may, if desired, be driven with broadband thermal light characterized by a mean photon number  $\bar{n}$ . Two stable

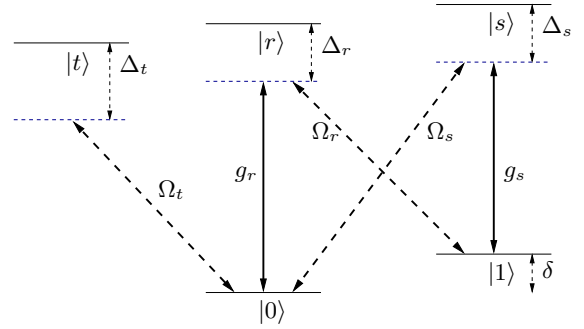


FIG. 1: Atomic level scheme for each atom. The excited states have energies  $\hbar\omega_j$  ( $j = r, s, t$ ).

ground states ( $|0\rangle, |1\rangle$ ) of each atom constitute the qubit states (Fig. 1). The cavity field and two auxiliary laser fields drive two separate resonant Raman transitions between these states. In particular, transitions  $|1\rangle \leftrightarrow |r\rangle$  and  $|0\rangle \leftrightarrow |s\rangle$  are driven by detuned laser fields with (real) Rabi frequencies  $\Omega_r$  and  $\Omega_s$  and relative phase difference  $\varphi$ , while the transitions  $|0\rangle \leftrightarrow |r\rangle$  and  $|1\rangle \leftrightarrow |s\rangle$  are strongly coupled to the cavity mode, with coupling strengths  $g_r$  and  $g_s$  (assumed the same for both atoms). Detunings of the fields from the excited states  $|r\rangle$  and  $|s\rangle$  are given by  $\Delta_r$  and  $\Delta_s$ . A fifth state  $|t\rangle$  is virtually excited from  $|0\rangle$  by another strongly detuned laser field, adding an additional ac-Stark shift to the state  $|0\rangle$ .

The master equation for the total system density operator is (taking  $\hbar = 1$ )

$$\dot{\rho} = -i[H, \rho] + \mathcal{L}_{\text{cav}}\rho + \mathcal{L}_{\text{spon}}\rho, \quad (1)$$

where  $H = H_{\text{cav}} + H_{\text{at}} + H_{\text{int}}$ , with  $H_{\text{cav}} = \omega a^\dagger a$ ,

$$\begin{aligned} H_{\text{at}} &= \sum_{i=1,2} \{ \omega_r |r_i\rangle \langle r_i| + \omega_s |s_i\rangle \langle s_i| + \omega_t |t_i\rangle \langle t_i| \\ &\quad + \delta |1_i\rangle \langle 1_i| + [(\Omega_r/2)e^{-i\omega_{L_r}t} |r_i\rangle \langle 1_i| + \text{H.c.}] \\ &\quad + [(\Omega_s/2)e^{-i[\omega_{L_s}t+\varphi]} |s_i\rangle \langle 0_i| + \text{H.c.}] \\ &\quad + [(\Omega_t/2)e^{-i\omega_{L_t}t} |t_i\rangle \langle 0_i| + \text{H.c.}] \}, \\ H_{\text{int}} &= \sum_{i=1,2} (g_r |r_i\rangle \langle 0_i| a + g_s |s_i\rangle \langle 1_i| a + \text{H.c.}), \quad (2) \end{aligned}$$

(H.c. denotes Hermitian conjugate) and

$$\begin{aligned} \mathcal{L}_{\text{cav}}\rho = & \kappa(1 + \bar{n}) (2a\rho a^\dagger - a^\dagger a\rho - \rho a^\dagger a) \\ & + \kappa\bar{n} (2a^\dagger \rho a - a a^\dagger \rho - \rho a a^\dagger). \end{aligned} \quad (3)$$

Here,  $\omega_{Lj}$  ( $j = r, s, t$ ) denote the laser frequencies. The term  $\mathcal{L}_{\text{spon}}\rho$  describes atomic spontaneous emission.

To isolate the essential dynamics, we assume large detunings of the light fields from the excited atomic states (i.e.,  $|\Delta_j| \gg \Omega_j, g_r, g_s, \kappa, \gamma_j$ , where  $\gamma_j$  is the linewidth of state  $|j\rangle$ ), so that atomic spontaneous emission is negligible and the excited states can be adiabatically eliminated from the problem. This leads to a reduced master equation for a pair of effective two-level atoms (involving states  $|0\rangle$  and  $|1\rangle$ ) coupled to the cavity mode. This reduced system is characterized by the parameters

$$\beta_j = g_j \Omega_j / (2\Delta_j), \quad \eta_j = g_j^2 / \Delta_j, \quad j = \{r, s\}, \quad (4)$$

where  $\beta_r$  and  $\beta_s$  are the two (Raman) coupling strengths, and  $\eta_r$  and  $\eta_s$  are the ac-Stark shifts per cavity photon induced in  $|0\rangle$  and  $|1\rangle$ , respectively.

To further reduce the model, we assume the ‘‘bad-cavity’’ limit,  $\kappa \gg |\beta_{r,s}|, |\eta_{r,s}|$ . This enables us to adiabatically eliminate the cavity mode, which yields a master equation for the atomic density matrix in the form

$$\begin{aligned} \dot{\rho} = & (2\beta^2/\kappa)(N+1) (2S\rho S^\dagger - S^\dagger S\rho - \rho S^\dagger S) \\ & + (2\beta^2/\kappa)N (2S^\dagger \rho S - S S^\dagger \rho - \rho S S^\dagger) \\ & - (2\beta^2/\kappa)M (2S^\dagger \rho S^\dagger - S^\dagger S^\dagger \rho - \rho S^\dagger S^\dagger) \\ & - (2\beta^2/\kappa)M^* (2S\rho S - S S\rho - \rho S S) \\ & + (\eta^2/2\kappa)\bar{n}(\bar{n}+1) (2P\rho P^\dagger - P^\dagger P\rho - \rho P^\dagger P). \end{aligned} \quad (5)$$

Here,  $\beta^2 = \beta_r^2 - \beta_s^2$ ,  $\eta^2 = (\eta_r - \eta_s)^2$ , and

$$N = \frac{(\bar{n}+1)\beta_s^2 + \bar{n}\beta_r^2}{\beta^2}, \quad M = \frac{-(2\bar{n}+1)\beta_r\beta_s e^{i\varphi}}{\beta^2}, \quad (6)$$

while  $S = (\sigma_1^- + \sigma_2^-) / \sqrt{2}$  and  $P = \sigma_1^- \sigma_1^+ + \sigma_2^- \sigma_2^+$  are collective atomic operators, with  $\sigma_i^- = |0_i\rangle\langle 1_i|$ .

The derivation of (5) also requires that the phase of the effective two-level system remains constant with respect to the laser phase difference  $\varphi$ . That is, the effective atomic system and squeezed reservoir must be ‘‘resonant’’ with each other, which requires that

$$\frac{\Omega_s^2}{4\Delta_s} - \frac{\Omega_r^2}{4\Delta_r} + \frac{\Omega_t^2}{4\Delta_t} + \frac{g_r^2}{\Delta_r} \bar{n} - \frac{g_s^2}{\Delta_s} \bar{n} = 0. \quad (7)$$

It is to satisfy this condition while retaining flexibility in our choices of  $\Omega_{r,s}$  and  $\Delta_{r,s}$  that we use the additional transition  $|0\rangle \leftrightarrow |t\rangle$ . The level shift  $\Omega_t^2/(4\Delta_t)$  provides an extra degree of freedom with which to satisfy (7).

In (5), the terms proportional to  $\beta^2$  describe the collective (amplitude) coupling of our pair of effective two-level

atoms to an effective squeezed reservoir, with the degree and purity of squeezing characterized by the parameters  $\{N, M\}$  [4, 5]. In particular, the effective squeezed quadrature variance is proportional to  $(N - |M| + 1/2)$  and ideal squeezing corresponds to  $|M|^2 = N(N+1)$ , which requires that  $\bar{n} = 0$ . The last line of (5) describes phase damping of the atomic qubits caused by coherent scattering of off-resonant (thermal) intracavity photons. There is no phase damping if  $\bar{n} = 0$  or if  $\eta_r = \eta_s$ .

A feature of the present system is that the strengths of the amplitude and phase damping terms are independently adjustable, so that, for example, one can be made to dominate the other (remembering that (7) must remain satisfied). Also, by switching off all sources of light (i.e., setting  $\beta_r = \beta_s = 0$  and  $\bar{n} = 0$ ) the state of the two-atom system can in principle be ‘‘frozen’’ at any instant.

To begin our analysis of (5), we note first that associated with the collective coupling of the atoms to the reservoir are certain decoherence-free states, which decouple completely from the dynamics [9]. In particular, defining  $|\phi^\pm\rangle = (|00\rangle \pm |11\rangle) / \sqrt{2}$  and  $|\psi^\pm\rangle = (|01\rangle \pm |10\rangle) / \sqrt{2}$ , one finds that  $|\psi^-\rangle$  decouples for all parameter choices, while  $|\psi^+\rangle$  decouples if  $N = M = 0$ .

As a first example, we consider the case in which phase damping can be neglected (i.e.,  $\eta = 0$  or  $\eta^2 \ll \beta^2$ ). The steady state density matrix  $\rho_{\text{ss}}$  is then, assuming an initial state that has no projection onto  $|\psi^-\rangle$ , given by

$$\rho_{\text{ss}} = \begin{pmatrix} \rho_{11} & 0 & 0 & \rho_{14} \\ 0 & \rho_{22} & \rho_{23} & 0 \\ 0 & \rho_{32} & \rho_{33} & 0 \\ \rho_{41} & 0 & 0 & \rho_{44} \end{pmatrix}, \quad (8)$$

specified in the basis  $\{|11\rangle, |10\rangle, |01\rangle, |00\rangle\}$ , with

$$\rho_{11} = \frac{|M|^2(1-2N) + N^2(1+2N)}{(1+2N)L}, \quad (9)$$

$$\rho_{22} = \rho_{33} = \rho_{23} = \frac{1}{6} - \frac{1}{6L}, \quad \rho_{14} = \frac{M}{(1+2N)L}, \quad (10)$$

where  $L = 1 + 3N(1+N) - 3|M|^2$ .

Examples of the steady state and time evolution to the steady state are shown in Figs. 2 and 3, respectively, plotted as points in the linear entropy-concurrence plane [10]. We plot a minor variation of the true definition of the concurrence and call it the *free concurrence*  $\mathcal{C}_{\text{free}} = (\lambda_1 - \lambda_2 - \lambda_3 - \lambda_4)$ , where  $\lambda_{1-4}$  are the square roots of the eigenvalues, in decreasing order, of  $\rho\tilde{\rho}$ , where  $\tilde{\rho} = (\sigma_y \otimes \sigma_y)\rho^*(\sigma_y \otimes \sigma_y)$ , with  $\sigma_y = -i(\sigma^+ - \sigma^-)$ . The use of the free concurrence enables separable states ( $\mathcal{C}_{\text{free}} \leq 0$ ) to be more readily distinguished. The linear entropy is given by  $S_L(\rho) = (4/3)[1 - \text{Tr}(\rho^2)]$ . On each graph we also plot lines corresponding to the Werner states,  $\rho_W = \xi|\phi^+\rangle\langle\phi^+| + (1/4)(1-\xi)\mathbf{1}_4$  ( $0 \leq \xi \leq 1$ ), the MEMS of [2], which have the maximum amount of entanglement for a given linear entropy, and thermal states  $\rho_{\text{th}} = [\zeta|0\rangle\langle 0| + (1-\zeta)|1\rangle\langle 1|]^{\otimes 2}$  ( $0 \leq \zeta \leq 1$ ). For ideal squeezing the

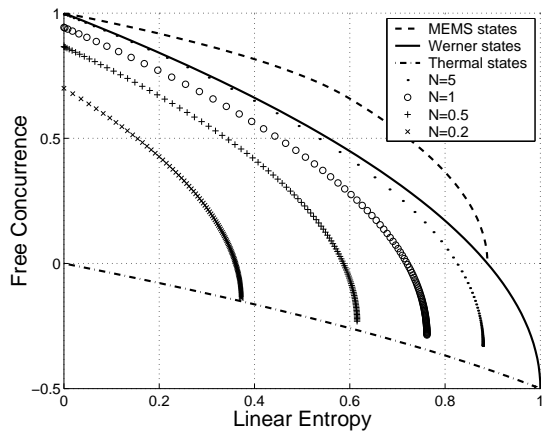


FIG. 2: Steady state values of  $\mathcal{C}_{\text{free}}(\rho)$  and  $S_L(\rho)$  for selected values of  $N$  and  $0 \leq |M|^2 \leq N(N+1)$ , for initial state  $|00\rangle$ .

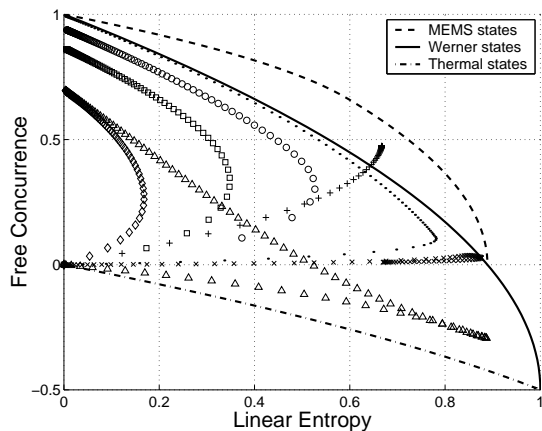


FIG. 3: Evolution of  $\mathcal{C}_{\text{free}}(\rho)$  and  $S_L(\rho)$  to the steady state with ideal squeezing ( $|M|^2 = N(N+1)$ ) for the following initial states and values of  $N$ :  $\{|00\rangle, N = 0.2\}$  ( $\diamond$ ),  $\{|00\rangle, N = 0.5\}$  ( $\square$ ),  $\{|00\rangle, N = 1\}$  ( $\circ$ ),  $\{|00\rangle, N = 5\}$  ( $\bullet$ ),  $\{|11\rangle, N = 0.2\}$  ( $\triangle$ ),  $\{|01\rangle, N = 2\}$  ( $\times$ ),  $\{|01\rangle, N = 0.01\}$  ( $+$ ). Note that the points on each curve are not equally spaced in time.

steady state described by (8) is the pure state [4]

$$|\Psi_s\rangle = \sqrt{\frac{N+1}{1+2N}} |00\rangle - e^{i\varphi} \sqrt{\frac{N}{1+2N}} |11\rangle. \quad (11)$$

These states lie on the left-hand vertical axes of the figures and approach the Bell states  $|\phi^\pm\rangle$  in the limit of large squeezing (i.e., large  $N$ , and  $\varphi = \pi$  or 0). Nonideal squeezing (Fig. 2) generates steady states that can lie essentially anywhere below the Werner line. Note that for large  $N$  the steady states closely approximate mixtures of  $|\phi^+\rangle\langle\phi^+|$  ( $\varphi = \pi$ ) and  $\rho' = \text{diag}\{1/3, 1/6, 1/6, 1/3\}$ .

Time evolution with ideal squeezing from initial states with zero projection onto  $|\psi^-\rangle$  can also sweep out the region beneath the Werner line (Fig. 3). When the initial state *does* have a projection onto  $|\psi^-\rangle$  (e.g.,  $|01\rangle$ ), an interesting range of points on the plane can also be accessed, including an area above the Werner line and the

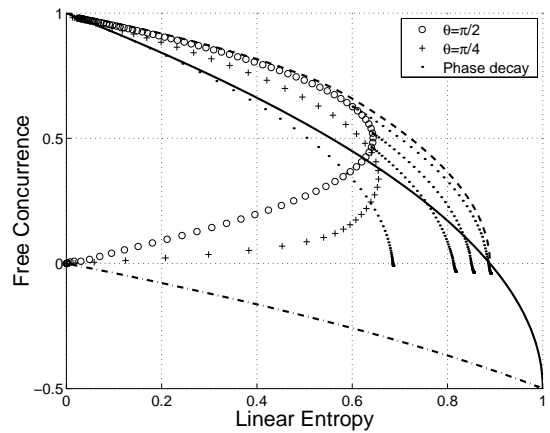


FIG. 4: Evolution of  $\mathcal{C}_{\text{free}}(\rho)$  and  $S_L(\rho)$  for initial states (12) with  $\theta = \{\pi/4, \pi/2\}$ ,  $N = 3.1$ , and  $\bar{n} = 0$ . The dotted curves show evolution produced by phase decay turned on after application of the unitary transformation  $U$  to a selection of states from the  $\theta = \pi/2$  curve. For this evolution, amplitude coupling is disabled, but  $\eta \neq 0$  and  $\bar{n} = 1$ .

region along the boundary at  $\mathcal{C}_{\text{free}} = 0$  between separable and entangled (including the maximally mixed entangled state at the intersection of the Werner and MEMS lines).

States above the Werner line can also be generated by initially preparing the separable pure superposition state

$$|\Psi(0)\rangle = \{\cos(\theta/2)\mathbb{1}_2 + i\sin(\theta/2)\sigma_y\}^{\otimes 2} |00\rangle, \quad (12)$$

with  $0 < \theta \leq \pi/2$ , and then applying the effective reservoir interaction with strong, ideal squeezing. In this case, the time evolution follows paths as shown in Fig. 4. There is a small region of the plane above the Werner line which cannot be reached by this method. However, this region can be accessed by switching off the squeezed reservoir interaction ( $\beta_{r,s} = 0$ ) and employing phase decay ( $\eta, \bar{n} \neq 0$ ) from initial states prepared on the  $\theta = \pi/2$  curve of Fig. 4 and to which the local unitary transformation  $U = (1/2)\{\sigma_x + \sigma_z\} \otimes \{\mathbb{1}_2 - i\sigma_y\}$  (requiring single-atom addressing with appropriate laser Raman pulses) has first been applied. This is also illustrated in Fig. 4.

We turn now to practical issues associated with our scheme. Analysis of (5) shows that the slowest rate featuring in the dynamics is  $(4\beta^2/\kappa)(2N - 2|M| + 1)$ , which exhibits the characteristic inhibited decay associated with atomic damping by a squeezed reservoir [11]. Meanwhile, inclusion of atomic spontaneous emission effects (due to finite excited state populations) into the model reveals characteristic rates  $\gamma_j(\Omega_j^2/2\Delta_j^2)$  ( $j = r, s, t$ ). Taking the rate for  $j = r$  to be the maximum, and setting  $\bar{n} = 0$ , the condition that spontaneous emission be negligible during the state preparation period reduces to  $2g_r^2/(\gamma_r\kappa) \gg [1 - \sqrt{N/(N+1)}]^{-2}$ . This amounts to the condition of strong coupling cavity QED, made somewhat more stringent however owing to the inhibited atomic decay rate. If we consider a recent cav-

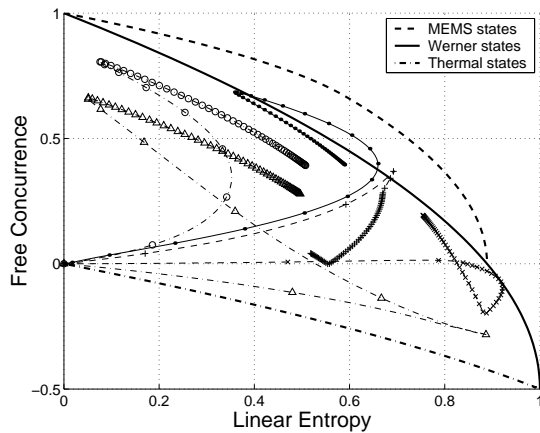


FIG. 5: Evolution of  $\mathcal{C}_{\text{free}}(\rho)$  and  $S_L(\rho)$  with spontaneous emission effects for  $(g_r, g_s, \kappa, \gamma_j, \Omega_s, \Delta_j)/2\pi = (110, 110, 14.2, 5.2, 100, 8000)$  MHz ( $j = r, s, t$ ),  $\Omega_t^2 = \Omega_r^2 - \Omega_s^2$ , and  $\bar{n} = 0$ , with the following initial states and values of  $\Omega_r$ :  $\{|00\rangle, \Omega_r = 173$  ( $N = 0.5$ ) $\}$  ( $\circ$ ),  $\{|11\rangle, \Omega_r = 245$  ( $N = 0.2$ ) $\}$  ( $\triangle$ ),  $\{|01\rangle, \Omega_r = 110$  ( $N = 5$ ) $\}$  ( $\times$ ),  $\{|01\rangle, \Omega_r = 458$  ( $N = 0.05$ ) $\}$  ( $+$ ). Note that the points are not equally spaced in time.

ity QED experiment for which the parameters achieved were  $(g, \kappa, \gamma)/2\pi = (110, 14.2, 5.2)$  MHz [12], then for  $N = 2$  the above inequality reads as  $332 \gg 30$ , indicating that sufficiently strong coupling is experimentally realistic for achieving significant levels of effective squeezing. Furthermore, setting, e.g.,  $\Omega_r/\Delta_r = 0.02$  and using the above parameters, the characteristic state preparation time is  $\lesssim 50 \mu\text{s}$ , which is orders of magnitude less than single-atom trapping times in tightly-confining optical dipole traps (see, e.g., [13, 14, 15, 16]).

In Fig. 5 we present sample evolutions from a model in which the excited atomic states have been adiabatically eliminated, but in which effects of spontaneous emission plus the cavity mode dynamics are included. Using the cavity QED parameters quoted above, we see that a large area of the linear entropy-concurrence plane can be accessed. With the inclusion of spontaneous emission, decay into the (weakly-coupled) state  $|\psi^-\rangle$  can occur for states with no initial projection onto  $|\psi^-\rangle$ . This limits the maximal attainable concurrence and in Fig. 5 leads also, for the cases with  $\langle \psi^- | \rho(0) | \psi^- \rangle = 0$ , to a very slow decay of  $\mathcal{C}_{\text{free}}(\rho)$  and increase in  $S_L(\rho)$  after rapid initial evolution to the optimal value of  $\mathcal{C}_{\text{free}}(\rho)$ . Note again though that the evolution can be frozen at any point by simply turning off all of the light fields. Note also that for the highest value of  $\mathcal{C}_{\text{free}}(\rho)$  attained in Fig. 5, one finds  $\langle \phi^+ | \rho | \phi^+ \rangle \simeq 0.9$ . Higher cavity finesses (i.e., lower  $\kappa$  values) improve the performance of the scheme further and should be accessible experimentally [17].

An alternative scheme for engineering the entropy and

concurrence can also be formulated using actual squeezed light to drive the cavity and just a single cavity-mediated Raman transition. Further, with nondegenerate squeezed light fields driving distinct cavities it is possible to engineer the states of distantly separated atoms [18].

The scheme presented here can also be used to prepare spin-squeezed states of a larger number of cavity-confined atoms [5]. While preparing this manuscript, we became aware of proposals for preparing such states which use essentially the same configuration as in this work, only not in the guise of quantum reservoir engineering [19].

In conclusion, we have proposed a scheme for engineering atomic two-qubit states with any allowed combination of linear entropy and concurrence. This should open the door to detailed experimental investigation of purity and entanglement in quantum information protocols.

We acknowledge helpful discussions with S. Rebić and W. J. Munro. This work was supported in part by the Marsden Fund of the Royal Society of New Zealand.

\* Corresponding author. Email address: s.parkins@auckland.ac.nz

- [1] A. G. White, D. F. V. James, W. J. Munro, and P. G. Kwiat, Phys. Rev. A **65**, 012301 (2001).
- [2] W. J. Munro, D. F. V. James, A. G. White, and P. G. Kwiat, Phys. Rev. A **64**, 030302 (2001).
- [3] N. Lütkenhaus, J. I. Cirac, and P. Zoller, Phys. Rev. A **57**, 548 (1998).
- [4] G. M. Palma and P. L. Knight, Phys. Rev. A **39**, 1962 (1989).
- [5] G. S. Agarwal and R. R. Puri, Opt. Commun. **69**, 267 (1989); Phys. Rev. A **41**, 3782 (1990).
- [6] R. F. Werner, Phys. Rev. A **40**, 4277 (1989).
- [7] E. Hagley *et al.*, Phys. Rev. Lett. **79**, 1 (1997).
- [8] S. Osnaghi *et al.*, Phys. Rev. Lett. **87**, 037902 (2001).
- [9] M. B. Plenio, S. F. Huelga, A. Beige, and P. L. Knight, Phys. Rev. A **59**, 2468 (1999).
- [10] Note that the concurrence  $\mathcal{C}$  is monotonically related to the entanglement of formation  $E_F(\rho)$ , i.e.,  $E_F(\rho) = h((1 + \sqrt{1 - \mathcal{C}^2})/2)$  where  $h(x) = -x \log_2 x - (1-x) \log_2 (1-x)$ .
- [11] C. W. Gardiner, Phys. Rev. Lett. **56**, 1917 (1986).
- [12] C. J. Hood *et al.*, Science **287**, 1447 (2000).
- [13] J. Ye, D. Vernooy, and H. J. Kimble, Phys. Rev. Lett. **83**, 4987 (1999).
- [14] R. Scheunemann, F. S. Cataliotti, T. W. Hänsch, and M. Weitz, Phys. Rev. A **62**, 051801(R) (2000).
- [15] D. Frese *et al.*, Phys. Rev. Lett. **85**, 3777 (2000).
- [16] N. Schlosser, G. Reymond, I. Protchenko, and P. Grangier, Nature **411**, 1024 (2001).
- [17] H. J. Kimble, private communication.
- [18] S. G. Clark and A. S. Parkins, unpublished.
- [19] A. André, L.-M. Duan, and M. D. Lukin, quant-ph/0107075; A. S. Sørensen and K. Mølmer, quant-ph/0202073.